

Field-enhancement properties of nanotubes in a field emission setup

Ch. Adessi

NASA Ames Research Center, Mail Stop: T27A-1, Moffett Field, California 94035-1000

M. Devel

Laboratoire de Physique Moléculaire, UMR CNRS 6624, 16 route de Gray, F-25030 Besançon Cedex, France

(Received 3 August 2001; published 1 February 2002)

The polarization phenomenon, involved in the mechanisms of emission from carbon nanotubes, is investigated by means of a self-consistent resolution of Poisson's equation. We show that the field enhancement, responsible for the emission, varies in a logarithmic way with the nanotube length. This leads, for most of the nanotubes investigated, to a rapid saturation of the amplification of the field which does not allow for the recovery of experimental values for microscopic lengths. However, this saturation is less important with $(n,0)$ nanotubes and values of the amplification factor around 2000 can be obtained with small diameter nanotubes of this kind. The case of nanotube films is also investigated, and the dependence of the amplification factor with the nanotube density is pointed out. Finally, the screening effect of the outer shells on the inner ones is investigated in the case of multiwall nanotubes.

DOI: 10.1103/PhysRevB.65.075418

PACS number(s): 85.35.Kt, 33.15.Kr, 85.45.Fd, 41.20.Cv

I. INTRODUCTION

Field emission from carbon nanotubes,¹⁻⁵ seems very promising for technological application such as flat panel displays. The requirements for such devices are a low turn-on field, a high brightness, a good dynamics, and a low cost. The materials considered so far for these devices range from Spindt-type tips⁶ to diamondlike films,⁷⁻¹⁰ or more recently, ultrathin semiconducting films (UTSC's).¹¹⁻¹³ Apart from UTSC's which have not been extensively tested yet for this application, most of the materials pose important technical problems, such as the uniformity of the emissive surface which is, at present, one of the most challenging problems. For example, no solution has been found yet to extend beyond about 5%, the emissive surface of diamondlike films. Actually, carbon nanotube films, with their low turn-on macroscopic field and their uniform surfaces (thanks to well controlled deposition techniques), represent serious candidates for flat panel displays. Several prototypes have even already been proposed.¹⁴⁻¹⁸

The turn-on field, under which no significant current is observed, is of the order of 3 V/ μm (Ref. 19) for multiwall nanotubes. One mechanism suspected to lead to this low-field-emission property is the very high enhancement of the field at the tip of the nanotubes, which would allow to obtain a high enough microscopic field at the emission sites with a rather low applied macroscopic field. This hypothesis has been partly verified with *ab initio* calculations for short nanotubes (≤ 10 nm).²⁰ However, the validity of these results for nanotubes longer than 10 nm is questionable. Moreover, they do not provide any explanation for the very large differences observed experimentally between apparently similar nanotubes. Furthermore, experimental and theoretical evidences have pointed out that localized states at the end of the tubes are involved in the emission process. In this context, the emission mechanism is still unclear and the respective implications of the field-enhancement factor and of lo-

calized states are still to be determined. For example, Han *et al.*²⁰ have shown that the enhancement of the field is due to the occupation of localized states at the end of the nanotubes and, on the other hand, Adessi *et al.*²¹ have shown that the electronic emission are mediated by localized states which do not seem to cause the enhancement of the field.

In order to elucidate the implication of the field-enhancement phenomenon in the field emission process, we have studied, by means of a self-consistent resolution of Poisson's equation, the evolution of the field-enhancement factor for various single wall (SWNT's), double wall, and triple wall nanotubes. These calculations have been performed by means of an atomic anisotropic dipolar approximation to model the induced deformation of the electronic cloud. It has allowed us to deduce the induced field at the end of the nanotubes for lengths up to 30 nm. Moreover, they have allowed us to extrapolate a diameter variation law of the field-enhancement factor and to conclude on the respective implications of the inner and outer shells of multiwall nanotubes (MWNT's) on the field-enhancement factor. In the following section, we will recall the basis of the method used to solve Poisson's equation. Then, we will present the results obtained for various SWNT's and MWNT's.

II. RESOLUTION METHOD

The aim of this method is to describe the effects induced by the surface and the applied field on the atoms of the nanotube. In first approximation, the deformation of the electronic cloud of a carbon atom can be modeled by using an anisotropic dipolar polarizability. However, to take into account the global response of the nanotube, it is necessary to compute the dipolar distribution self-consistently by resolution of Poisson's equation. Inside the volume of a neutral nanotube, Poisson's equation then reads

$$\begin{aligned}
\Delta V(\vec{r}) &= -\frac{\rho(\vec{r})}{\epsilon_0} = \frac{1}{\epsilon_0} \vec{\nabla} \cdot \vec{P} \\
&= \vec{\nabla}_r \cdot [\vec{\chi}(\vec{r}) \vec{E}(\vec{r})] \\
&= \vec{\nabla}_r \cdot \left[\sum_{j=1}^{N_{at}} \vec{\alpha}_j \delta(\vec{r} - \vec{r}_j) \vec{E}(\vec{r}) \right], \quad (1)
\end{aligned}$$

where \vec{P} is the dipolar momentum per unit volume, $\vec{\chi}(\vec{r})$ the local dielectric susceptibility, $\vec{E}(\vec{r})$ the electric field, and $\vec{\alpha}_j$ the anisotropic polarizability tensor of the j th carbon atoms. $V(\vec{r})$ is then solution of

$$V(\vec{r}) = V_0(\vec{r}) + \int d^3r' G_0(\vec{r}, \vec{r}') \vec{\nabla}_{r'} \cdot \sum_{j=1}^{N_{at}} \vec{\alpha}_j \delta(\vec{r}' - \vec{r}_j) \vec{E}(\vec{r}'), \quad (2)$$

where $G_0(\vec{r}, \vec{r}')$ is the generalized Green's function of the Laplacian satisfying the limit conditions of the problem. It is proportional to the electrostatic potential at the point \vec{r} , due to the presence of a test charge at the point \vec{r}' . Its expression is: $G_0(\vec{r}, \vec{r}') = -1/4\pi\|\vec{r} - \vec{r}'\| + \Delta/4\pi\|\vec{r} - \vec{r}'^*\|$, where Δ represents the reflection coefficient of the surface (equal to 1 for a perfect metal), and \vec{r}'^* the symmetric of \vec{r}' with respect to the surface.

Integrating this equation by parts, and using $\vec{E}(\vec{r}) = -\vec{\nabla}V(\vec{r})$, this can be restated in Lippmann-Schwinger's form:

$$\vec{E}(\vec{r}) = \vec{E}_0(\vec{r}) + \sum_{j=1}^{N_{at}} \vec{S}_0(\vec{r}, \vec{r}_j) \cdot \vec{\alpha}_j \cdot \vec{E}(\vec{r}_j), \quad (3)$$

where $\vec{S}_0(\vec{r}, \vec{r}') = \vec{\nabla}_r \vec{\nabla}_{r'} G_0(\vec{r}, \vec{r}')$ represents the electrostatic field propagator associated with the reference system, i.e., a half metallic space bounded by the plane $z=0$ and N_{at} the number of atoms. By substituting the N_{at} vectors \vec{r}_i for \vec{r} in the self-consistent Eq. (3) one simply gets a linear system of $3 \times N_{at}$ unknowns, namely the components of the N_{at} vectors $\vec{E}(\vec{r}_i)$, which can be solved by standard dense matrix solvers. The potential can then be computed anywhere by making use of Eq. (2), once integrated by parts.

III. NUMERICAL RESULTS

In all the presented results, the system considered corresponds to a nanotube physisorbed on a perfect metallic surface (with $\Delta=1$, as defined in the previous section) at a distance of 2.6 Å.²² In this system, the induced effects of the counter electrode are not considered. This approximation is done in order to focus on the influence of the intrinsic properties of the nanotubes.

The present method, in contrast to *ab initio* ones, allows to investigate nanotubes with more than 4000 atoms. It corresponds, for nanotubes of diameter of the order of 1 nm, to lengths up to 35 nm. The accuracy of this method has already been tested in the case of a C₆₀ fullerene physisorbed on a surface.²³ Thus It has been possible to study, by a systematic investigation, the main factors influencing the enhancement

of the applied field in a field-emission setup.

In this paper, we have tried to answer some relevant questions about field emission from carbon nanotubes. Actually, experimental evidences have shown that the emission from carbon nanotube films occurs only from very few nanotubes and that most of the surface does not emit. In order to increase the current density, one possibility is to increase the nanotube density. However, this solution tends to decrease the field-enhancement phenomenon.²⁴ Another more practical possibility is to increase the number of emitting nanotubes. For this purpose, one must first answer why most of the nanotubes do not emit. One common hypothesis to explain this nonuniform emission is that only the longer nanotubes, for which the enhancement of the field is the most important, emit. However, the validity of this hypothesis depends mainly on the evolution of the β factor with the length of the nanotubes.

Another question linked with these kind of emitters is the realism of the very large values (up to 10 000) of the field-enhancement factor (or β factor) measured by some authors.²⁵ However, these values are extracted from I-V characteristics with a Fowler-Nordheim model, which is normally only valid for plane metallic electrodes. Furthermore, the β values quoted also depend on the value of the work function used. Conversely, in the present study, the β factor is calculated directly by the ratio of the maximum value of the local field, on the tube axis near its end, by the applied field. Thus it allows us to verify to which extent the values obtained experimentally with the work function of amorphous carbon are realistic.

The last relevant question we have tried to answer here is the influence of the nanotube density in nanotube films on the field-enhancement factor. Actually, a simple model using uniform metallic tubes²⁴ clearly shows that an increased density of nanotubes lowers β , so that there is an optimum density. This is confirmed experimentally in the same paper with a study of films with varying densities. However, these results have to be checked with a more realistic model.

A. Single wall nanotubes

The first point investigated here is the evolution of the β factor with the length of various SWNT's. Actually, Han *et al.*²⁰ point out that this evolution is linear, at least up to 10 nm, leading to values as large as the biggest ones observed experimentally, when extrapolated to lengths of the order of 1 μm. However, Fig. 1 shows that, for our test nanotubes, this linear relation does not hold any more for nanotubes longer than 5–15 nm. On each subfigure, the evolution with length of the β factor for a (n,n) and a $(n,0)$ nanotube with close diameters are compared. From left to right, we compare a (6,0) with a (3,3), a (9,0) with a (5,5), and a (12,0) with a (7,7). First, one can notice that a saturation of the β factor with the length of the nanotubes seems to occur for all the nanotubes, but it is clearly faster for (n,n) nanotubes. One other remark concerns the evolution with the diameter. We can clearly notice that the β factor decreases when the diameter of the tube increases. This observation is coherent

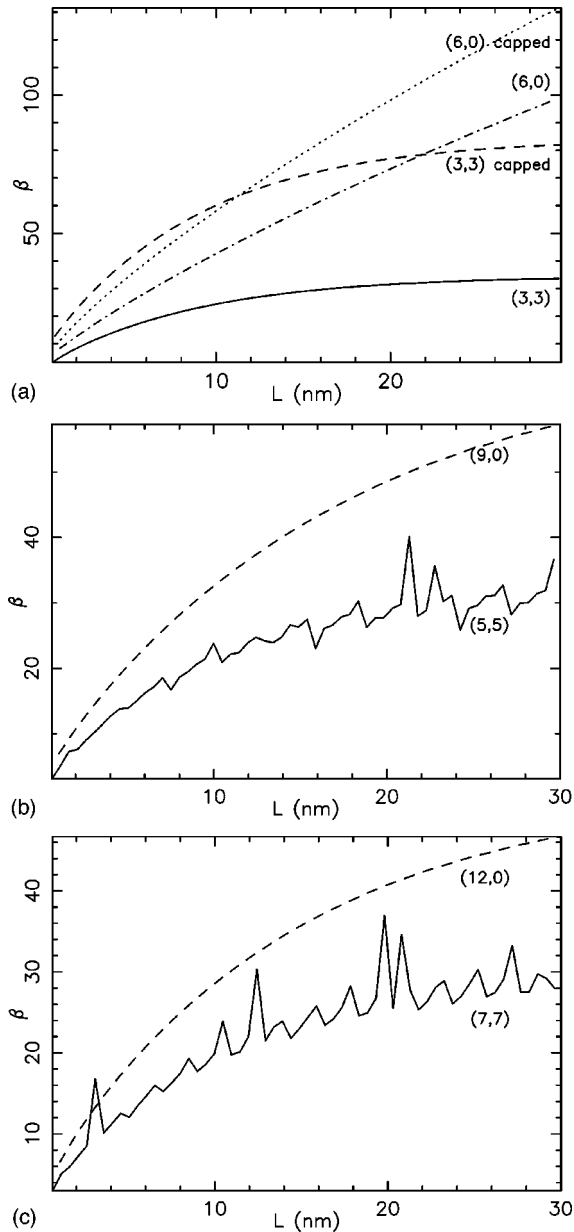


FIG. 1. Evolution of the field-enhancement factor (denoted β) with the length of the nanotubes. In the three figures, we have represented together the curves corresponding to a (n,n) and a $(n,0)$ nanotube with close diameters. The indices of each tubes are denoted in the vicinity of the corresponding curve. For the top figure, the nanotubes referred to as “capped” correspond to nanotubes ended with a closed structure. One can notice the saturation of the β factor with the length.

with the results obtainable with a uniform metallic cylinder²⁶ for which the enhancement of the field is proportional to the inverse power of the diameter of the cylinder. However, we can notice that the saturation phenomenon occurs for shorter nanotube lengths when the diameter is increased.

The third remark concerns the significantly different behavior of (n,n) nanotube and $(n,0)$ nanotubes. Actually, $(n,0)$ nanotubes seem to be the best field amplifier and the saturation phenomenon occurs for lengths greater than for (n,n) nanotubes. This difference could originate in the align-

ment of the applied field with some of the C-C bonds in the $(n,0)$ nanotube which is never the case for (n,n) ones. For example, the $(6,0)$ nanotube with a diameter of 0.47 nm has a β factor of 100, for a length of 30 nm, whereas the $(3,3)$ nanotube with a diameter of 0.41 nm has a β factor of only 34 despite its smaller diameter. In order to check the validity of this conclusion when the nanotubes are capped, we have also considered the case when the $(3,3)$ and the $(6,0)$ nanotubes are capped with a hexagon. As expected, the caps increase the enhancement of the field by approximately a factor 2. However, the general trend of each nanotube is not affected and the saturation, observed with the $(3,3)$, remains. This trend can be fitted with a logarithmiclike series of general expression: $\beta(L) = L \times [a_0 + a_1 \ln(L) + a_2 \ln^2(L) + \dots]$. However, it cannot be used to extrapolate our curves for longer lengths due to large uncertainties. Thus, in order to nevertheless have some comparison points with experimental data, we have used a linear approximation using only the last points of our curves to extrapolate the value of the β factor for a length of 1 μm . We obtain for the open $(6,0)$ nanotube a value of the order of 1900, and of the order of 3100 for the closed one. We note that these values are of the same order of magnitude than the best experimental ones, for which the structure of the emitting nanotube is not known.

On Fig. 2 is represented the evolution of the β factor with the diameter for $(n,0)$ nanotubes, first for 30-nm-long nanotubes, second for the same nanotubes but after linear extrapolation to a length of 1 μm (which corresponds to a length commonly observed experimentally). We have tried to extract a general trend and the best fit is obtained with a series of rational functions of general expression: $\beta(D) = \Sigma(a_n/D^n)$. The main point which can be drawn from this curve is that β values around 2000 can be reached for nanotubes with diameters of the order of 0.5 nm. These large values of the β factor are, however, lower than those reported experimentally for SWNT. Moreover, the $(9,0)$ nanotube, which is the smallest nanotube which can be observed isolated, leads to a β factor only of the order of 600 which is not comparable with experimental values. For example, the turn-on field (leading to a current density of 10 $\mu\text{A}/\text{cm}^2$) reported by Bonard *et al.* in Ref. 19 for a SWNT film is 2.7 V/ μm . Using a simple Fowler-Nordheim model³⁵ such field would lead, with the β factor of the $(9,0)$ nanotube, to a current density of only 4×10^{-5} $\mu\text{A}/\text{cm}^2$. Actually, nanotubes with smaller diameters are only observed as the inner shell of multiwall nanotubes,^{27,28} or after very special preparation that has still not been applied to field emission. To justify these differences with experimental values one could argue that the work function used to extract the amplification factor with a Fowler-Nordheim model is an overestimation of the real work function for carbon nanotubes. However, one more realistic explanation is probably the omission, in our simulations, of the effect of the counter electrode for which a significant role has been pointed out recently.²⁹

In order to point out the implications of the chirality of the nanotubes on the β factor, we have compared three SWNT's with close diameters but different chiral angles. In Fig. 3 is plotted the β factor for a $(10,0)$, $(9,2)$, and $(8,3)$ nanotube with respective diameters of 0.78, 0.79, and 0.77

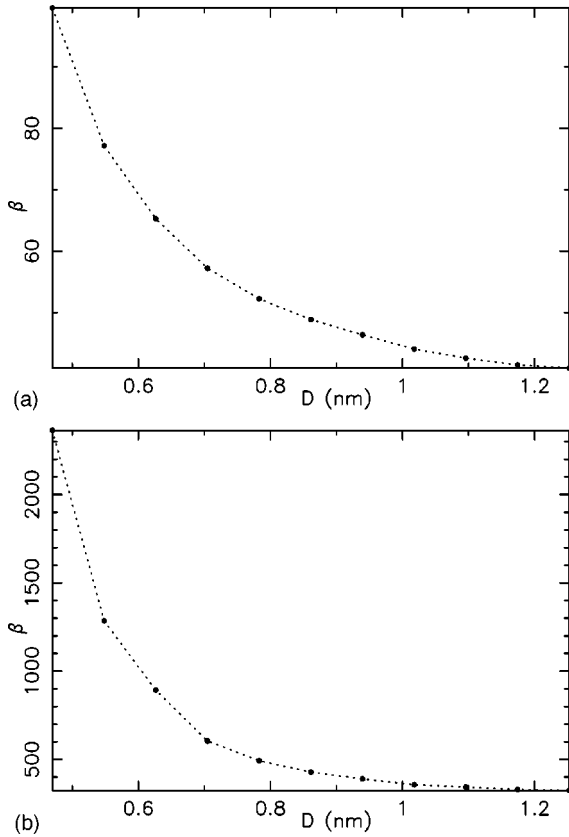


FIG. 2. Evolution of the field-enhancement factor (denoted β) with the diameter of $(n,0)$ nanotubes. The top figure corresponds to the results of our calculation for 30-nm-long $(n,0)$ nanotubes. The bottom figure corresponds to an extrapolation for a length of 1 μm . Large values of the β factor are obtained only for diameters smaller than 0.5 nm.

nm and chiral angle of 0.0, 9.8, and 15.3°, respectively. On this figure, the main noticeable variation with the chiral angle is the increasing instability of the β factor which occur when the chiral angle increases. However, as will be developed in the next section, this oscillatory behavior tends to disappear for multiwall nanotubes. One explanation of this instability of the β factor may be the large period of chiral nanotubes. Actually, for the range of nanotube lengths considered here, we do not have a finite number of period conversely to achiral nanotubes for which the length increment can only be done by a half period. However, it is not possible to conclude here that the chirality plays a significant role on the variation of β factor.

So as to check the influence of the nanotube density on the β factor, we have considered a $(6,0)$ nanotube film in a closed pack arrangement and measured the evolution of the field with the mesh parameter (denoted a). In Fig. 4 is represented the evolution of the β factor when the interaction with the first and second neighbors are taken into account. When a is large (greater than 10 nm), β tends to the value observed with an isolated nanotube (approximately 33 for the given nanotube length). Conversely, the more the mesh parameter decreases, the more the β factor decreases (in accordance with the result obtain in Ref. 24). However, for

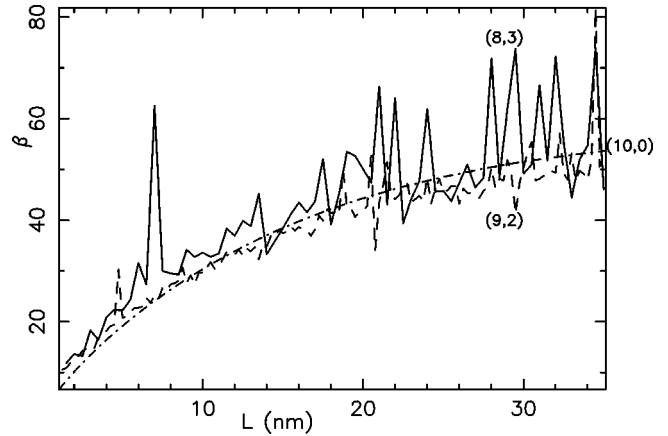


FIG. 3. Evolution of the field-enhancement factor (denoted β) with the length of the nanotubes. In this figure, we have represented the curves corresponding to a $(8,3)$, a $(9,2)$, and a $(10,0)$ nanotube (solid, dashed, and dash-dotted lines, respectively) which have close diameters and different chiral angles. It can be seen that the chiral angle only affects the smoothness of the curve but not its general trend.

mesh parameter of 1 nm, the β factor is only lowered by approximately a factor 2 which is a rather low screening effect compared with the one observed by Nilsson *et al.* This result shows that the nanotube density, even if it has a lowering effect, does not modify drastically the β factor and the difference pointed out between (n,n) and $(n,0)$ nanotubes is more significant.

In Fig. 5 is represented a contour plot of the polarization potential for a rope of 13 $(6,0)$ nanotubes in a close-packed arrangement, corresponding to the system used to compute the β factor with second neighbor interactions represented in Fig. 4. The screening effect of the external nanotubes over the central one is clearly noticeable in this figure. This effect leads to the decrease of the β factor observed in Fig. 4 when

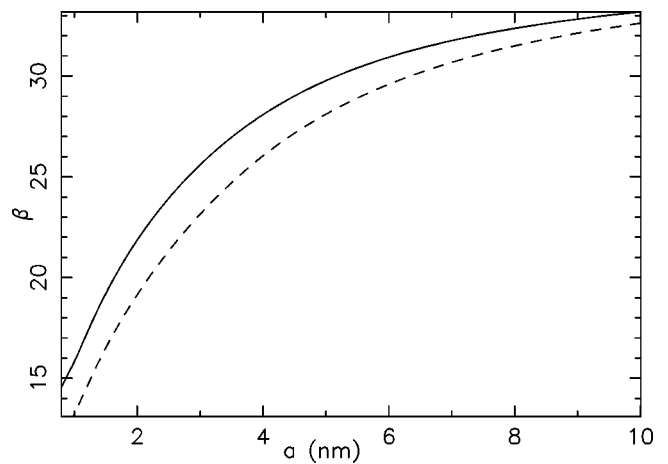


FIG. 4. Evolution of the field-enhancement factor (denoted β) with the mesh parameter of a $(6,0)$ nanotube film in a close-packed arrangement. The length of the tubes is 7 nm. For the solid line, we have only considered the interaction with the first nearest neighbors. For the dashed line, the second nearest neighbors are also considered.

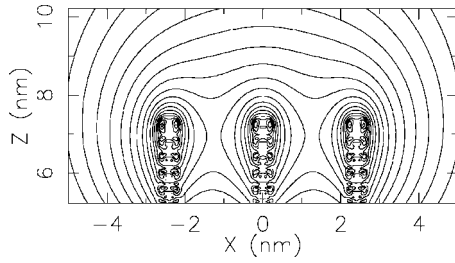


FIG. 5. Contour map of the polarization potential in the plane X - Z for a system constituted by 13 (6,0) nanotubes in a close-packed arrangement. The spacing between two isopotentials is 450 meV. In this figure one can see the central nanotube surrounded by two of its first neighbors. As expected, the enhancement of the field is larger close to the brim of the rope.

the nanotube density is increased. However, the most interesting point is the large difference observed between the potential map in the vicinity of the external nanotubes and this of the central one. Actually, the isopotentials are closer near the external nanotubes. This behavior is also observed with MWNT's,²⁶ with diameters of the order of several nanometers, when they are described as uniform metallic conductors. It is observed in Ref. 26 that the field tends to be larger in the vicinity of the brim of the nanotube. In such a situation, the electronic emission is coming mainly from the external nanotubes and not from the central one. This situation is encountered experimentally with patterned nanotube films obtained by a printing method for which the emission occurs mainly from the brim of the blocks, leading to a large opening of the emitted beam. To avoid such a situation it is clear that a low nanotube density is preferable.

It is important to point out that in all the presented results, there is no noticeable influence of the band structure (and therefore of the electronic conduction properties) of nanotubes. This is not surprising considering that these results are obtained with a local dipolar model. Moreover, the occurrence of the polarization phenomenon described here leads to the field enhancement, but does not imply any charge displacement. However, the conduction properties of the nanotube depends on the band structure of the nanotubes and thus an additional contribution on the electron emission properties can be expected.

B. Multiwall nanotubes

Nowadays, one of the most widely used techniques to produce nanotube films is chemical vapor deposition (CVD). However, the production of SWNT's by a similar technique³⁰ has been done only quite recently and most of the experimental observations done with nanotube films produced by a CVD technique involve MWNT's. Moreover, β factors reported for MWNT's (Ref. 31) with diameters of a few nanometers are smaller than for SWNT's but, of the order of 1000. This seems contradictory with our results for SWNT's. Actually, we argue that β factors of the order of 1000 may be obtained only with $(n,0)$ nanotubes with diameter smaller than 0.5 nm. Thus one could wonder whether the field-

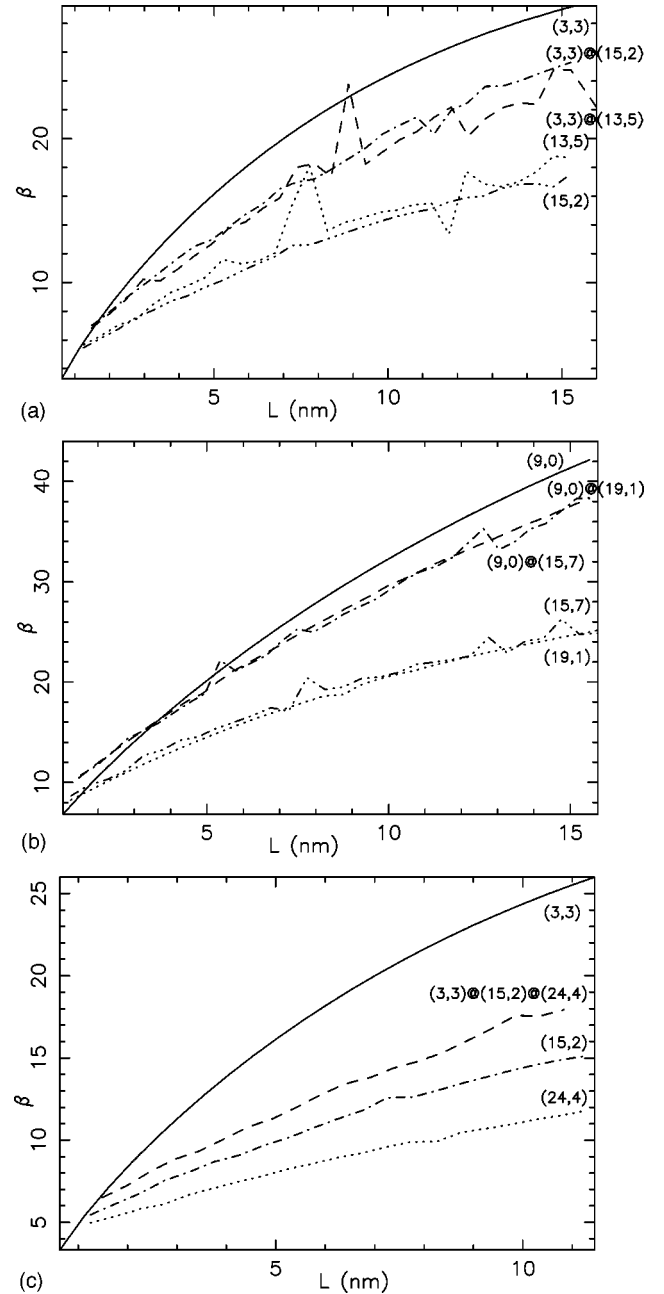


FIG. 6. Evolution of the field-enhancement factor (denoted β) with the length of the nanotubes. In the top figure, we have represented the plots corresponding to two double wall nanotubes constituted by a (3,3) inner shell with a (15,2) or (13,5) outer shell. In the central figure, we have represented the plots corresponding to two double wall nanotubes constituted of a (9,0) inner shell with a (19,1) or (15,7) outer shell. In the bottom figure, we have represented a triple wall nanotube constituted of a (3,3) inner shell with a (15,2) middle shell and a (24,4) outer shell. In each figure we have added the plot corresponding to the different shell alone for comparison. The outer shells act as Faraday cages over the inner shells, but the enhancement of the field is still mainly due to the inner shells.

enhancement property of MWNT's is due to the presence of small diameter inner shells. In such a case, the lower amplification factor observed with MWNT's might originate from a screening of the applied field by the outer shells. To answer

these questions, we have checked the evolution of the β factor with length for various MWNT's.

In Fig. 6 are represented the evolution, with length, of the β factor for four double wall nanotubes (left and central figures) and one triple wall nanotube (right figure). In all the cases, the shells have been chosen accordingly to the inter-shell spacing \hat{d}_{002} measured in Ref. 32. The double wall nanotubes are constituted by a (9,0) and a (3,3) inner shell for the left and central figures, respectively, with two different outer shells each. On these two figures, the two respective outer shells have approximately the same diameter [for the (3,3) the outer shells have a diameter of 1.26 nm and for the (9,0) the outer shells have a diameter of 1.53 nm]. The major difference between the two respective outer shells is their chiral angle. However, due to their rather large diameter, there is no significant difference between their β factors. When we compare the curves for the isolated nanotubes with the ones for double wall nanotubes, the clear effect of the outer shells over the inner one is a lowering of the total field enhancement.

This effect is also noticeable in the right side of Fig. 6 which corresponds to the evolution of the β factor with the length of a triple wall nanotube constituted by a (3,3) inner shell, a (15,2) middle shell, and a (24,4) outer shell. It can be noticed that the β factor of this triple wall is higher than the one for the middle shell. Thus, even with three shells, the β factor is mainly set by the inner shell. However, the β factor for this triple wall nanotube is smaller than the one for the same nanotube without the outer shell [i.e., the (3,3)@(15,2) used for the left figure]. Thus the addition of a third shell tends to decrease the β factor as is expected, knowing that carbon nanotubes are good Faraday cages.³³ Actually, for a length of 10 nm the β factor for the (3,3)@(15,2) is 21 and for the (3,3)@(15,2)@(24,4) is 17. These results seem to indicate that the good emission properties of MWNT's reported experimentally would be due only to a few inner shells and that most of the outer shells would have few implications in the field-enhancement mechanism.

IV. CONCLUSION

We show that for carbon nanotubes, the field-enhancement property, which corresponds to a polarization phenomenon, can be modeled by means of a dipolar approximation, however, giving results independent of the band structure (and therefore of the electronic conduction properties) of the nanotube.

In the case of opened nanotubes, large differences are observed between (n,n) and ($n,0$) nanotubes. We show that only ($n,0$) nanotubes with small diameters (≤ 0.5 nm) can lead to high values of the amplification factor. However, we have not obtained values as large as those observed experimentally and this would tend to prove that factors other than polarization are involved in the mechanism of emission. These results are not much affected when capped nanotubes are considered. Actually, caps improve the field amplification factor (approximately by a factor 2) but the polarization mechanism and the saturation phenomenon remain unchanged.

We show, in the case of nanotube films, that an increase in the nanotube density decreases only slightly the β factor. In the case of a rope of nanotubes, we clearly show that the field amplification is larger on the external tubes than on the central one. This effect is observed experimentally and leads to an emission by the brim of the blocks.

Finally, we argue that the field amplification properties of MWNT are due to inner shells with small diameters. We base this conclusion on the evolution of the β factor with the diameter observed with SWNT's.

ACKNOWLEDGMENTS

We would like to thank J.-M. Bonard for helpful comments and discussions. This work was partly supported by the Washington State University under the NASA Cooperative Agreement No. NCC2-5407, and by the "région de Franche-Comté" under Contract No. 2001-BS70.

¹A. Rinzler, J. Hafner, P. Nikolaev, L. Lou, S. Kim, D. Tománek, P. Nordlander, D. Colbert, and R. Smalley, *Science* **269**, 1550 (1995).

²W. de Heer, A. Châtelain, and D. Ugarte, *Science* **270**, 1179 (1995).

³P. Collins and A. Zettl, *Appl. Phys. Lett.* **69**, 1969 (1996).

⁴S. Fan, M. Chapline, N. Franklin, T. Tomblor, A. Cassell, and H. Dai, *Science* **283**, 512 (1999).

⁵J.-M. Bonard, H. Kind, T. Stöckli, and L.-O. Nilson, *Solid-State Electron.* **45**, 893 (2001).

⁶C. Spindt, *Appl. Phys. Lett.* **39**, 3504 (1968).

⁷M. Geis, J. Twichell, J. Macaulay, and K. Okano, *Appl. Phys. Lett.* **67**, 1328 (1995).

⁸K. Okano, S. Koizumi, S. Silva, and G. Amaratunga, *Nature (London)* **381**, 140 (1996).

⁹M. Geis, J. Twichell, and T. Lyszczarz, *J. Vac. Sci. Technol. B* **14**, 2060 (1996).

¹⁰M. Geis, N. Efremow, K. Krohn, J. Twichell, T. Lyszczarz, R. Kalish, J. Greer, and M. Tabat, *Nature (London)* **393**, 431 (1998).

¹¹Vu Thien Binh and C. Adessi, *Phys. Rev. Lett.* **85**, 864 (2000).

¹²Vu Thien Binh, J. Dupin, P. Thevenard, S. Purcell, and V. Semet, *J. Vac. Sci. Technol. B* **18**, 956 (2000).

¹³Vu Thien Binh, J. Dupin, C. Adessi, and V. Semet, *Solid-State Electron.* **45**, 1025 (2001).

¹⁴Q. Wang, A. Setlur, J. Lauerhaas, J. Dai, E. Seelig, and R. Chang, *Appl. Phys. Lett.* **72**, 2912 (1998).

¹⁵W. Choi, D. Chung, J. Kang, H. Kim, Y. Jin, L. Han, Y. Lee, J. Jung, N. Lee, G. Park and J. Kim, *Appl. Phys. Lett.* **75**, 3129 (1999).

¹⁶S. Fan, W. Liang, H. Dang, N. Franklin, T. Tomblor, M. Chapline, and H. Dai, *Physica A* **8**, 179 (2000).

¹⁷D. Chung, W. Choi, J. Kang, H. Kim, I. Han, Y. Park, Y. Lee, N.

- Lee, J. Jung, and J. Kim, *J. Vac. Sci. Technol. B* **18**, 1054 (2000).
- ¹⁸Q. Wand, M. Yan, and R. Chang, *Appl. Phys. Lett.* **78**, 1294 (2001).
- ¹⁹J.-M. Bonard, J. Salvétat, T. Stöckli, L. Forró, and A. Châtelain, *Appl. Phys. A: Mater. Sci. Process.* **69A**, 245 (1999).
- ²⁰S. Han and J. Ihm, *Phys. Rev. B* **61**, 9986 (2000).
- ²¹C. Adessi and M. Devel, *Phys. Rev. B* **62**, R13 314 (2000).
- ²²P. Graviil, M. Devel, P. Lambin, X. Bouju, C. Girard, and A. Lucas, *Phys. Rev. B* **53**, 1622 (1996).
- ²³M. Devel, C. Girard, and C. Joachim, *Phys. Rev. B* **53**, 13 159 (1996).
- ²⁴L. Nilsson, O. Groening, C. Emmenegger, O. Kuettel, E. Schaller, L. Schlapbach, H. Kind, J.-M. Bonard, and K. Kern, *Appl. Phys. Lett.* **76**, 2071 (2000).
- ²⁵J.-M. Bonard, J. Salvétat, T. Stöckli, W. de Heer, L. Forró, and A. Châtelain, *Appl. Phys. Lett.* **73**, 918 (1998).
- ²⁶L. Wei, W. Baoping, T. Linsu, Y. Hanchun, and T. Yan, *J. Vac. Sci. Technol. B* **18**, 2704 (2000).
- ²⁷L.-C. Qin, X. Zhao, K. Hirahara, Y. Miyamoto, Y. Ando, and S. Iijima, *Nature (London)* **408**, 50 (2000).
- ²⁸N. Wang, Z. Tang, G. Li, and J. Chen, *Nature (London)* **408**, 50 (2000).
- ²⁹N.S. Xu, Y. Chen, S.Z. Deng, J. Chen, X.C. Ma, and E.G. Wang, *J. Phys. D* **34**, 1597 (2001).
- ³⁰J.-F. Colomer, C. Stephan, S. Lefran, G. Van Tendeloo, I. Willems, Z. Kónya, A. Fonseca, and J.B. Nagy, *Chem. Phys. Lett.* **317**, 83 (2000).
- ³¹J.-M. Bonard F Maier, T. Stöckli, A. Châtelain, W. de Heer, J. Salvétat, and L. Forró, *Ultramicroscopy* **73**, 7 (1998).
- ³²C.-H. Kiang, M. Endo, P. Ajayan, G. Dresselhaus, and M. Dresselhaus, *Phys. Rev. Lett.* **81**, 1869 (1998).
- ³³C. Girard, M. Devel, X. Bouju, and P. Graviil, in *Atomic and Molecular Wires*, Vol. 341 of *NATO Advanced Science Studies, Series E: Applied Sciences*, edited by C. Joachim and S. Roth (Kluwer Academic, Dordrecht, 1997), pp. 179-192.
- ³⁴D. Lovall, M. Buss, E. Graugnard, R.P. Andres, and R. Reifenberger, *Phys. Rev. B* **61**, 5683 (2000).
- ³⁵To estimate the emitted current we have used the equation used in Ref. 26 with a work function of 5.1 eV (Ref. 34).